JOURNAL OF Materials CHEMISTRY

X-Ray powder diffraction study of a new vanadium oxide $Cr_{0.11}V_2O_{5.16}$ synthesized by a sol–gel process

Gilles Grégoire, Noël Baffier,* Andrée Kahn-Harari and Jean-Claude Badot

Ecole Nationale Supérieure de Chimie de Paris, Laboratoire de Chimie Appliquée de l'Etat Solide (UMR CNRS 7574), 11 rue Pierre et Marie Curie, 75231 Paris Cedex 05, France

The synthesis of the mixed oxide $Cr_{0.11}V_2O_{5.16}$, which presents interesting electrochemical performances, has been performed from vanadium oxide gels. Its structure, determined by Rietveld refinement, is similar to that of orthorhombic V_2O_5, with the formation of CrO_6 short chains linking the V_2O_5 layers. For comparison, the structures of V_2O_5 (synthesized by the sol–gel route) and $Fe_{0.11}V_2O_{5.16}$ have been also determined by the same method. The position, along the *c* axis, of the trivalent ion in the plane formed by the four oxygen atoms of the V_2O_5 slab, is discussed as a function of the ion size and the crystal field stabilization energy.

Starting from molecular precursors to obtain an oxide network, the sol–gel process has drawn much attention as a method leading to a better control of the synthesis, particularly in the case of transition metal oxides.[1] Various textures (monodispersed powders, thin films, fibers) can be obtained directly from the solution at lower temperatures than through the usual solid state reaction.[2]

Vanadium pentoxide gels have been extensively studied during the past.[3] They exhibit a layered structure suitable for ionic and molecular intercalation reactions. Many applications have been evidenced according to the electronic or ionic properties of the ion inserted materials. Among these, an application as a reversible cathode in lithium batteries has been reported, insofar as the redox potential of the V^{5+}–V^{4+} couple is >3 V relative to the Li–Li^+ couple.[4] The oxide $Fe_{0.11}V_2O_{5.16}$ has been synthesized from vanadium pentoxide gels.[5] This new compound exhibits an orthorhombic symmetry close to that of the vanadium pentoxide V_2O_5, but its electrochemical behavior differs. For example, instead of the sharp voltage change observed for $x=1$ in $Li_xV_2O_5$, a smooth continuous potential decrease ensures the transition from the first insertion step near 3.2 V to the third around 2.3 V. In addition, an attractive cycling lifetime was found with this new oxide for a high depth discharge.[5,6] In order to attempt to explain this behavior, the structure of $Fe_{0.11}V_2O_{5.16}$ was determined by the Rietveld procedure.[7] The structure can be described by the same layers as V_2O_5, with the iron atoms located at the center of the square plane formed by the four oxygen atoms of the V_2O_5 slab. Two extra oxygen atoms complete the trivalent iron octahedral environment. As the iron ion is connected to neighboring iron *via* one extra oxygen atom, this results in the presence of chains $(Fe\text{-}O)_n$ perpendicular to the V_2O_5 slabs. Owing to charge balancing considerations, the FeO_6 octahedra are arranged to form only short chains along the *c* axis. Mössbauer and EPR spectroscopies[8] have confirmed that iron atoms are essentially octahedral. These structural features result in V_2O_5 layers linked to each other in the *c* direction through Fe—O groups, increasing the three-dimensional character of the phase and leading to a higher stability of the host lattice during lithium electrochemical cycling.

The present paper deals with the X-ray powder diffraction study of the analogous chromium compound $Cr_{0.11}V_2O_{5.16}$ which presents a still better electrochemical cyclability than the iron compound and the parent oxide V_2O_5.[9] Its structure has been determined from the Rietveld method in a Bragg–Brentano geometry (reflection) by using flat plate samples. In order to compare our results with those obtained on the iron compound with the same Rietveld method but in a Debye–Scherrer geometry using a Lindeman capillary[6] (transmission), we have also refined the structure of the iron compound $Fe_{0.11}V_2O_{5.16}$ and that of V_2O_5 orthorhombic oxide obtained from sol–gel synthesis under the same conditions.

Synthesis procedure

Vanadium pentoxide sols were prepared *via* the acidification of a sodium metavanadate solution $NaVO_3$ (0.1 M) through a column loaded with a proton exchange resin (Dowex 50W-X2, 50-100 mesh).[10] A yellow solution of decavanadic acid was initially obtained which polymerizes slowly to a dark red gel. The resulting gel exhibits an entangled fibrous structure, resembling flat ribbons about 10 Å thick.[11] The ribbons have a structure similar to that of orthorhombic V_2O_5.[11–14] The gel was spread into a thin layer on a glass plate and after drying at room temperature a xerogel corresponding to the composition $V_2O_5{\cdot}1.6\ H_2O$ was obtained. Its X-ray diffraction (XRD) pattern in reflection geometry shows a series of 00*l* peaks resulting from one-dimensional ordering perpendicular to the platelet: the *d*-spacing is about 11.60 Å, corresponding to a single interfoliar water layer (2.8 Å thick). The ribbons are negatively charged, with *ca.* 0.3–0.4 *e* charge per V_2O_5. This charge is compensated by 0.3–0.4 H_3O^+ ions leading to ionic exchange properties between the H_3O^+ cations and other charged species such as, *e.g.*, M^{m+} cations.[15]

The following step consists in the synthesis of $M_xV_2O_5{\cdot}nH_2O$ ($M=Cr^{3+}$, Fe^{3+}) xerogels by ionic exchange. Intercalation of the transition metal ions is realized by direct immersion of a V_2O_5 xerogel sample in a 0.1 M solution of $M(NO_3)_3$. This reaction is complete within 20 min. The XRD pattern in reflection geometry shows that the intercalation of cations between xerogel ribbons preserves the initial preferred orientation (one-dimensional ordering associated with the stacking of ribbons upon each another). Nevertheless, the *d*-spacing between the xerogel ribbons, which is about 14.10 Å for Fe^{3+}, is 14.40 Å for Cr^{3+} and greater than for the xerogel (11.60 Å). This difference is observed because the M^{3+} intercalated compounds contain two water layers.[16]

Simultaneous thermogravimetric analysis (TGA) and differential scanning calorimetry (DSC) were carried out with a heating rate of 10 K min^{-1}, in an atmosphere of flowing argon using a Netzsch STA 409 instrument equipped with data manipulation software. The TG curve of the $Cr_xV_2O_5{\cdot}nH_2O$ xerogel shows three mass loss stages (Fig. 1): stage 1, *ca.*

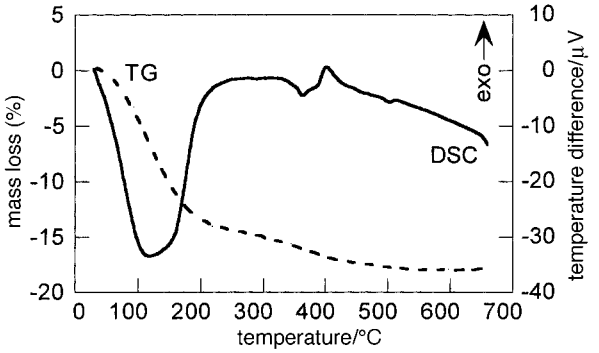

Fig. 1 Simultaneous thermogravimetric analysis (TGA) and differential scanning calorimetry (DSC) of $Cr_xV_2O_5{\cdot}nH_2O$ xerogel

20–200 °C, is accompanied by a large endothermal peak and can be attributed to the loss of a weakly bonded water (1.68 H_2O per mole). Stage 2, *ca.* 200–350 °C, is accompanied by a small endothermal peak and it corresponds to the removal of the interfoliar water (0.44 H_2O per mole). Stage 3, *ca.* 350–450 °C, is accompanied by a small endothermal signal. This mass loss corresponds to the progressive departure of strongly bound water (0.22 H_2O per mole). Finally crystallization occurs near 410 °C and gives an orthorhombic phase close to V_2O_5. The total amount of water determined by thermal analysis is *ca.* 2.34 H_2O per mole.

The last step consists in the preparation of vanadium pentoxide V_2O_5 and mixed vanadium chromium or iron oxides $M_xV_2O_{5+y}$. These oxides are prepared by thermal treatment of the corresponding xerogels (550 °C for V_2O_5 and 520 °C for $M_xV_2O_{5+y}$). The cation contents have been determined by atomic emission spectroscopy (induced coupled plasma). The oxidation states of vanadium and iron or chromium have been deduced from chemical redox titration. The results lead, for the mixed oxides, to formulae $M_{0.11}V_2O_{5.16}$ in which the oxidation states of vanadium and of chromium or iron are 5 and 3 respectively. These compounds can thus be considered as the combination V_2O_5–$0.055M_2O_3$. Consequently, it will be necessary to take into account the presence of 0.16 additional oxygen atoms per chemical formula to ensure the charge balance of the structural arrangement of the mixed oxides.

X-Ray powder diffraction analysis

The X-ray powder diffraction study was performed with a Bragg–Brentano geometry, using flat plate samples with a Siemens D 5000 diffractometer, equipped with Co-Kα radiation and a back graphite monochromator. The XRD diagrams of the compounds show strong preferential orientation along the *c*-axis perpendicular to the film surface for the $M_{0.11}V_2O_{5.16}$ compounds (only the 00*l* peaks are present) and in the *ab* plane for V_2O_5 oxide (only the *hk*0 peaks are present). Although successive grindings were performed, the particle sizes were still too large and random orientation was not sufficiently achieved to minimize preferential orientation. Eventually it was necessary to sieve the oxide powder to 20 μm through a nylon sieve and under these conditions preferential orientation effects were minimized. By using March's function, the residual effect could be accounted for in the Rietveld procedure. The powder diffraction pattern was scanned by steps of 0.01°(2θ), with fixed counting times (20 s). After data collection, the stability of the X-ray source and of the sample were checked by remeasuring the first few lines of the pattern.

Structure refinement procedure

Powder pattern indexing

The precise determination of peak positions was carried out by means of the Socabim fitting program PROFILE, available in the PC software package DIFFRACT-AT supplied by Siemens. The powder patterns of vanadium pentoxide V_2O_5 and iron– or chromium–vanadium oxide $M_{0.11}V_2O_{5.16}$ were indexed by means of the computer program U-FIT.[17]

Structure refinement procedure

Rietveld refinement[18] was performed by using the FULLPROF program.[19] Peak shapes were described by Pearson VII functions. The angular dependence of the peak full width at half maximum (FWHM) was described by the usual quadratic form in tan(θ)[20]

$$\mathrm{FWHM}^2 = U\tan^2\theta + V\tan\theta + W$$

where U, V and W are fitting parameters. The background intensity was evaluated by a polynomial expression for which the coefficients were refined. The refinement was carried out within the angular range $17 < 2\theta < 100°$.

First, a whole pattern matching procedure was applied in order to extract angular positions and integrated intensities from the powder diffraction pattern. No structural model was introduced in the process,[21] but instead, the profile parameters (unit cell, cosθ shift, peak shape and background intensity parameters) were refined. Integral intensities were distributed over three FWHM on either side of a diffraction line profile. The output data were then used as input data in the Rietveld refinement.

The Rietveld procedure requires an initial structural model. V_2O_5 structure refinement was started with the model proposed by Enjalbert and Galy[22] from single crystal investigations. Furthermore, intercalation of iron or chromium ions into V_2O_5 leads to a compound very close to the V_2O_5 structure. For this reason, we have assumed that both vanadium and oxygen atoms were located in the same positions of the *Pmmn* space group as in V_2O_5. Under these conditions, we must consider the large number of refinable parameters ($\approx$30) with respect to the experimental data ($\approx$80 Bragg peaks). The Rietveld procedure which we chose consisted in refining non-structural and structural parameters separately. Only non-structural parameters were initially refined: scale factor, coefficient of the background polynomial, cosθ shift parameter, three unit cell constants, three half width parameters and three profile shape function (Pearson VII) parameters which were progressively introduced into the calculation.

In the second stage, these non-structural parameters were then fixed and the refinement involved structural parameters : atomic coordinates and displacement factors.

The final stage consisted in progressively introducing both non-structural and structural parameters into the profile analysis refinement. The last variable to be refined was the preferred-orientation factor by using a March's function. Because of their correlation, scale factor and occupancy factors were not refined at the same time.

This refinement procedure was used for each compound, but the number of refinable parameters is different between vanadium pentoxide and iron– or chromium–vanadium oxide.

Results and Discussion

Recall on the structure of V_2O_5

V_2O_5 has an orthorhombic layered structure built up from square pyramids [VO_5] sharing edges and corners, leading to V_2O_5 sheets linked together *via* weak vanadium–oxygen interactions parallel to the *c*-direction.[23] The most recent structural

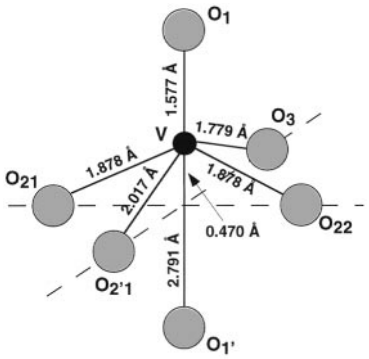

Fig. 2 Situation of the vanadium atom in the VO_5 polyhedron of V_2O_5 structure after Enjalbert and Galy (ref. 22)

determination is that of Enjalbert and Galy[22] from a single crystal study involving 450 measured unique reflections. From these results, it was shown that the vanadium atom located within the oxygenated coordination polyhedron VO_5 is shifted towards the plane formed by four oxygen atoms by a distance of 0.470 Å (Fig. 2). The sum of the shortest $V-O_1$ distance (1.577 Å) and of the longest $V-O_{1'}$ distance (2.791 Å) binding the chains of VO_5 polyhedra along the *c*-direction corresponds to the *c*-lattice constant (4.368 Å). The existence of a weak $V-O_{1'}$ bond gives vanadium a '5+1' coordination and V_2O_5 can be described as a combination of very distorted VO_6 octahedra.[23]

The chromium compound $Cr_{0.11}V_2O_{5.16}$

With regard to its chemical formula, as for the iron compound $Fe_{0.11}V_2O_{5.16}$, the unit cell of the chromium compound $Cr_{0.11}V_2O_{5.16}$ contains, in addition to the four independent atoms (1 V and 3 O) of V_2O_5, one Cr atom with partial occupancy of 0.11 and one independent oxygen atom with partial occupancy of 0.16.

30 parameters, including 12 structural parameters, were refined in the final cycle, based on 74 reflections ($17^\circ < 2\theta < 100^\circ$) (Table 1). The cell constants of $Cr_{0.11}V_2O_{5.16}$ are listed in Table 2. For comparison, we have also listed the cell parameters of the iron compound $Fe_{0.11}V_2O_{5.16}$ and those

Table 1 Details of Rietveld refinements for V_2O_5 and $M_{0.11}V_2O_{5.16}$ (M = Fe, Cr)

	V_2O_5 sol–gel	$Fe_{0.11}V_2O_{5.16}$	$Cr_{0.11}V_2O_{5.16}$
space group		*Pmmn*	
Z (number of unit formulae)		2	
wavelength (Å)		1.78897 ($K\alpha_1$), 1.79285 ($K\alpha_2$)	
step (2θ/°); time per step (s)		0.01; 20	
2θ range/°		17–100	
number of reflections		74	
number of independent atoms	4	5	5
number of structure parameters	11	12	12
number of profile parameters	18	16	18
R_B[a]	0.051	0.077	0.054
R_F[b]	0.046	0.059	0.040
R_p[c]	0.177	0.282	0.278
R_{wp}[d]	0.244	0.297	0.294

[a] $R_B = \sum_k |I_k(\text{obs}) - I_k(\text{calc})| / \sum_k |I_k(\text{obs})|$. [b] $R_F = \sum_k |(I_k(\text{obs}))^{1/2} - (I_k(\text{calc}))^{1/2}| / \sum_k (I_k(\text{obs}))^{1/2}$. [c] $R_p = \sum_i |y_i(\text{obs}) - y_i(\text{calc})| / \sum_i |y_i(\text{obs})|$. [d] $R_{wp} = \left(\frac{\sum_i \omega_i [y_i(\text{obs}) - y_i(\text{calc})]^2}{\sum_i \omega_i [y_i(\text{obs})]^2} \right)^{1/2}$.

Table 2 Values of the unit cell constants for sol–gel and monocrystal V_2O_5, and for $M_{0.11}V_2O_{5.16}$ compounds (M = Fe, Cr)

compound	*a*/Å	*b*/Å	*c*/Å	*V*/Å^3
monocrystal V_2O_5[22]	11.512(3)	3.564(1)	4.368(1)	179.214
sol–gel V_2O_5	11.5125(5)	3.5640(2)	4.3713(2)	179.357
$Fe_{0.11}V_2O_{5.16}$	11.540(1)	2.5629(3)	4.3500(3)	178.854
$Cr_{0.11}V_2O_{5.16}$	11.4849(5)	3.5635(5)	4.3817(3)	179.327

of sol–gel and monocrystal V_2O_5. With regard to the cell parameters of the iron compound, we have observed for the chromium compound a slight decrease of the *a*-lattice constant (11.485 Å *cf.* 11.540 Å) and a slight increase of *c* (4.382 Å *cf.* 4.350 Å) corresponding to an increase of the unit cell volume. The *b*-parameter, characteristic of the short distances V—O—V, is unchanged (3.563 Å). From these results, as for $Fe_{0.11}V_2O_{5.16}$, the chromium atoms were located in the 2b sites, almost at the center of the average plane formed by four oxygen atoms of the V_2O_5 slab: O_{21} and $O_{2'2}$ shared by three VO_5 polyhedra, O_3 and $O_{3'}$ shared by two VO_5 polyhedra (Fig. 3). Two oxygen atoms, O_4 and $O_{4'}$, had to be added along with the Cr ions, along the *c*-direction, to ensure an octahedral oxygen environment for the chromium atom, with a distance $O_4-Cr-O_{4'}$ equal to the *c* value (4.382 Å). Fig. 4 shows the fit obtained between the calculated and the observed patterns for $Cr_{0.11}V_2O_{5.16}$. Final convergence was obtained with the following *R*-values: $R_B = 0.0538$ and $R_F = 0.0402$, which are very satisfactory. However, the corresponding values for profile R_p and weight-profile R_{wp} factors are much higher: $R_p = 0.278$, $R_{wp} = 0.294$. These latter results may be explained by two factors, the first due to a relatively inappropriate evaluation of the background in relation with the experimental

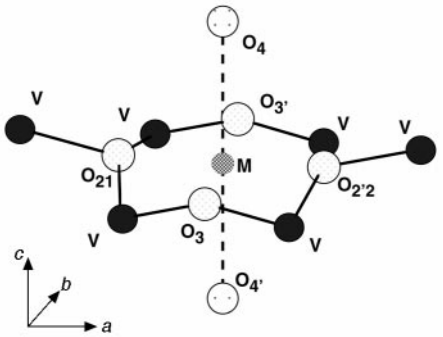

Fig. 3 Perspective view of the average plane formed by the four oxygen atoms $O_{21}O_3O_{2'2}O_3$ of the V_2O_5 slab, and the position of the inserted M atom with the two additional oxygen atoms O_4 and $O_{4'}$

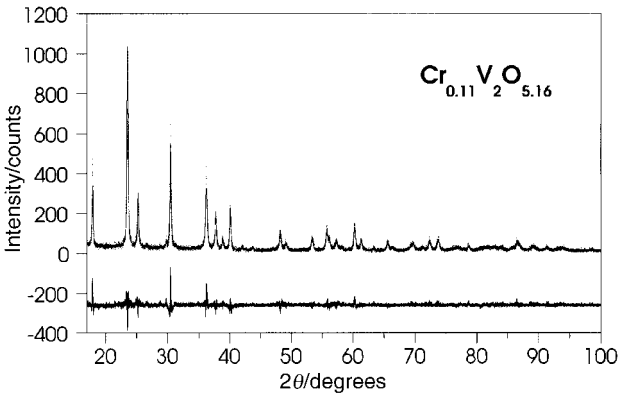

Fig. 4 Final Rietveld difference plots for the chromium compound $Cr_{0.11}V_2O_{5.16}$. The upper trace shows the observed data as dots, while the calculated pattern is represented by solid line. The lower trace is a plot of the difference: observed minus calculated.

Table 3 Positional parameters (x, y, z) and thermal parameters (B_{iso}) for the iron compound $Fe_{0.11}V_2O_{5.16}$ and for the chromium compound $Cr_{0.11}V_2O_{5.16}$

$Fe_{0.11}V_2O_{5.16}$					
atom	position	x/a	y/b	z/c	B_{iso}/Å^2
V	4f	0.3970(3)	0.25	0.0950(5)	3.8(2)
O1	4f	0.3972(8)	0.25	0.473(2)	4.2(3)
O2	4f	0.5648(6)	0.25	0.989(2)	0.9(3)
O3	2a	0.25	0.25	−0.001(2)	1.5
Fe	2b	0.75	0.25	0.044(5)	1
O4[a]	2b	0.75	0.25	0.5	
$Cr_{0.11}V_2O_{5.16}$					
atom	position	x/a	y/b	z/c	B_{iso}/Å^2
V	4f	0.3976(3)	0.25	0.1055(5)	3.1(1)
O1	4f	0.3968(8)	0.25	0.465(1)	2.8(2)
O2	4f	0.5689(7)	0.25	0.995(1)	2.4(3)
O3	2a	0.25	0.25	0.005(2)	1.5
Cr	2b	0.75	0.25	0.011(6)	1
O4[a]	2b	0.75	0.25	0.5	

[a]Additional oxygen not introduced into the calculation completing the Fe^{3+} or Cr^{3+} octahedral environment.

procedure, the second due to the limited number of available peaks (74) in relation with the number of parameters to be fitted (30). Nevertheless, the satisfactory results obtained for the Bragg factors R_B and R_F lead us to think that the Rietveld refinement is acceptable. The final atomic positions and displacement parameters are given in Table 3. Selected interatomic distances and angles are listed in Table 4. A perspective view of the structure of $Cr_{0.11}V_2O_{5.16}$ is shown in Fig. 5. As for the iron compound, the chromium atoms are located in 2b crystallographic sites, with two extra oxygen atoms apart from the average plane of the four oxygen atoms of the V_2O_5 slab. In the same way, according to the charge balance of the chemical formulae, only 11% of Cr^{3+} sites are occupied, thus leading to the existence of short CrO_6 octahedral chains along the c-axis.

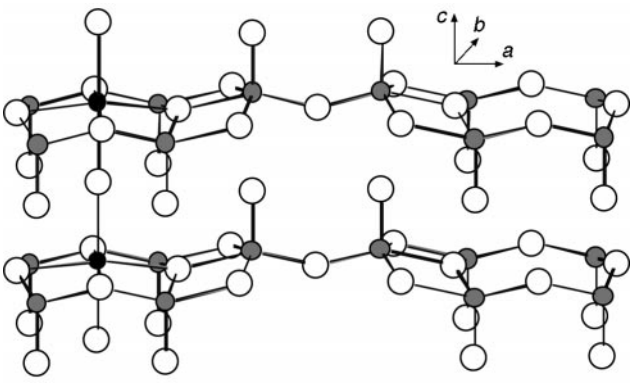

Fig. 5 Perspective view of $Cr_{0.11}V_2O_{5.16}$ structure: the Cr^{3+} ion, which is located within the slabs of V_2O_5, has an octahedral environment. Grey circles, V^{5+} ions; white circles, O^{2-} ions; black circles, Cr^{3+} ions. Not all Cr^{3+} sites are occupied.

Discussion

The octahedral environment for M^{3+} ions in $M_{0.11}V_2O_{5.16}$ (M = Fe, Cr) has been confirmed by a previous Mössbauer study for the iron compound.[8] As reported above, the trivalent ion is located at the center of the average plane formed by the four oxygen atoms O_{21}, $O_{2/2}$, O_3, $O_{3'}$ of the V_2O_5 slab, with two additional oxygen atoms O_4 and $O_{4'}$ located apart from the plane, along the c-direction, characterized by a distance $O_4-M-O_{4'}$ equal to the c-parameter value. Such an environment for the trivalent ion corresponds to $V^{5+}-M^{3+}-V^{5+}$ distances equal to 4.919(5) Å, *i.e.* a distance $V^{5+}-M^{3+}$ equal to 2.512(6) Å. Comparing this result with the shortest distance $V^{5+}-V^{5+}$ in the V_2O_5 oxide [3.092(5) Å], one can conclude that the interatomic M−V distances are large enough to allow a localization of the M^{3+} ion in the plane formed by the four oxygen atoms of the V_2O_5 slab. Fig. 6 shows the oxygen environment of the M^{3+} ions in the $M_{0.11}V_2O_{5.16}$ compounds as well as the same type of environment which would occur in V_2O_5. In the latter case, we have considered a fictive M atom at the center of the oxygen plane and two additional fictive

Table 4 Selected distances (Å) and angles (°) for $Fe_{0.11}V_2O_{5.16}$ and $Cr_{0.11}V_2O_{5.16}$[a]

$Fe_{0.11}V_2O_{5.16}$									
V	O_1	O_3	O_{21}	O_{22}	$O_{2/1}$	$O_{1'}$	Fe	O_4	$O_{4'}$
O_1	**1.644(9)**	2.67(1)	2.721(9)	2.721(9)	2.86(1)	4.3500(3)	3.24(2)	4.896(8)	2.463(6)
O_3	*103.9(5)*	**1.747(4)**	2.783(5)	2.783(5)	3.633(7)	2.85(1)	1.791(3)	2.815(7)	2.808(7)
O_{21}	*101.2(3)*	*100.5(2)*	**1.871(3)**	3.5629(3)	2.328(9)	2.97(1)	2.151(7)	3.084(8)	3.015(8)
O_{22}	*101.2(3)*	*100.5(2)*	*144.4(5)*	**1.871(3)**	2.328(9)	2.97(1)	4.162(4)	4.712(5)	4.668(5)
$O_{2/1}$	*103.3(4)*	*152.8(4)*	*74.1(2)*	*74.1(2)*	**1.991(8)**	2.96(1)	4.049(6)	4.571(7)	4.616(7)
$O_{1'}$	*179.9(7)*	*76.2(3)*	*78.7(3)*	*78.7(3)*	*76.6(3)*	**2.706(9)**	3.33(2)	2.464(6)	5.101(8)
Fe	*103.9(5)*	*45.0(1)*	*56.1(2)*	*56.1(2)*	*126.6(3)*	*76.2(5)*	**2.533(6)**	2.37(2)	1.98(2)
O_4	*136.5(2)*	*50.6(2)*	*59.7(2)*	*116.4(3)*	*107.1(2)*	*43.6(1)*	*32.6(5)*	**3.571(2)**	4.3500(3)
$O_{4'}$	*54.4(2)*	*66.1(2)*	*71.7(2)*	*71.7(2)*	*132.9(2)*	*125.6(2)*	*49.4(5)*	*82.1(1)*	**3.026(2)**
$Cr_{0.11}V_2O_{5.16}$									
V	O_1	O_3	O_{21}	O_{22}	$O_{2/1}$	$O_{1'}$	Cr	O_4	$O_{4'}$
O_1	**1.575(5)**	2.63(1)	2.719(5)	2.719(5)	2.85(1)	4.3817(3)	3.22(2)	4.888(5)	2.458(6)
O_3	*104.2(5)*	**1.751(4)**	2.739(6)	2.739(6)	3.663(8)	2.91(1)	1.783(1)	2.841(7)	2.807(7)
O_{21}	*103.6(2)*	*98.0(3)*	**1.876(2)**	3.5635(5)	2.38(1)	2.988(5)	2.081(8)	3.037(6)	3.005(6)
O_{22}	*103.6(2)*	*98.0(3)*	*143.7(4)*	**1.876(2)**	2.38(1)	2.988(5)	4.127(4)	4.682(4)	4.661(4)
$O_{2/1}$	*104.2(4)*	*151.6(3)*	*75.2(3)*	*75.2(3)*	**2.026(9)**	3.050(9)	4.073(7)	4.614(7)	4.635(7)
$O_{1'}$	*179.5(6)*	*75.3(3)*	*76.5(2)*	*76.5(2)*	*76.4(2)*	**2.807(5)**	3.36(2)	2.458(6)	5.156(5)
Cr	*101.5(6)*	*45.2(1)*	*54.3(3)*	*54.3(3)*	*127.4(3)*	*78.1(6)*	**2.512(6)**	2.14(3)	2.24(3)
O_4	*136.9(3)*	*50.4(2)*	*57.0(2)*	*113.1(2)*	*106.2(1)*	*42.7(1)*	*35.4(6)*	**3.618(2)**	4.3817(3)
$O_{4'}$	*54.7(2)*	*66.3(3)*	*71.8(2)*	*71.8(2)*	*133.2(1)*	*125.0(2)*	*46.8(6)*	*82.3(1)*	**3.006(2)**

[a]Bold values correspond to distances between the vanadium atom and the atom of the column. Each angle (in italics) corresponds to the angle formed by atom of the line, the vanadium atom and the atom of the column.

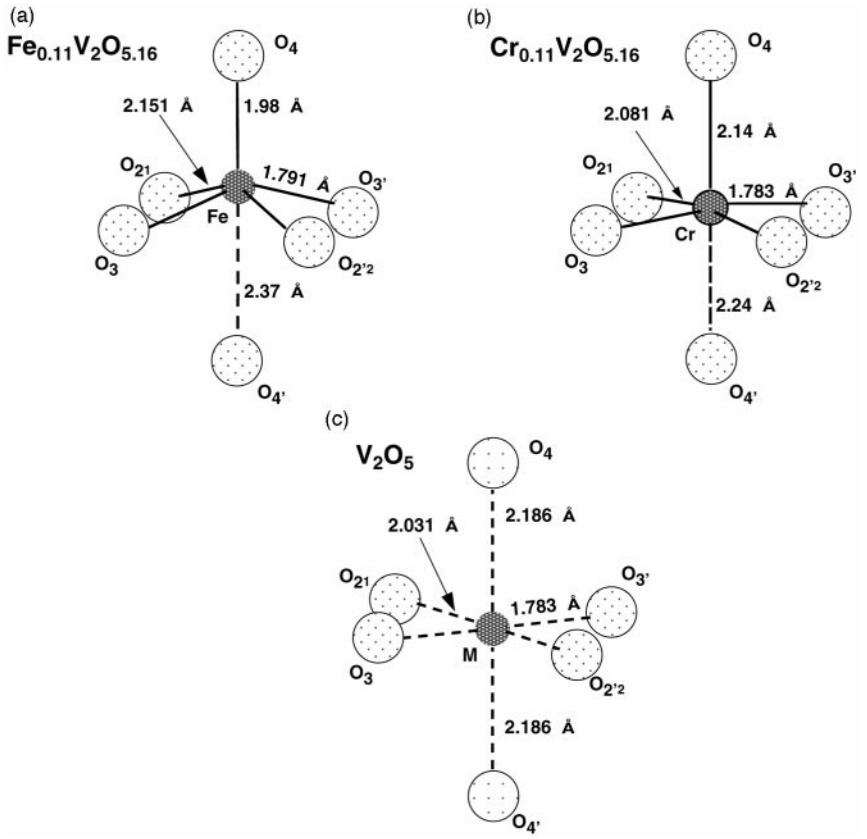

Fig. 6 Position of the trivalent M^{3+} ion into the MO_6 octahedron, for the iron compound (a) and for the chromium compound (b). Fig. 6(c) shows the same fictive environment which could correspond to the sol–gel V_2O_5 (two fictive additional oxygen atoms O_4 and $O_{4'}$ apart from the oxygen plane have been added at a distance of $c = 4.372$ Å from each other). The corresponding M—O distances are given.

oxygen atoms apart from the M atom at a distance of $c/2 =$ 2.186 Å. The corresponding distances are indicated in Fig. 6 and listed in Table 5. The various M—O distances should be compared with the values of the ionic radii of Fe^{3+} and Cr^{3+} given by Shannon[24] in relation with the coordination number and with the corresponding bond lengths $M^{3+}—O^{2-}$ indicated in Table 5. The atomic coordinates z of the different atoms (O, V, M) of the polyhedra are also listed in Table 5. For the chromium compound, the chromium ion [$z = 0.011(6)$] is virtually located in the plane formed by the four oxygen atoms ($z \approx 0$) of the V_2O_5 slab. For the iron compound, the iron ion lies off the oxygen plane [$z = 0.044(5)$] and is close to the plane formed by the four vanadium atoms ($z \approx 0.10$).

Table 5 (*a*) Values of the M—O distances (Å) corresponding to the oxygen octahedral environment of the trivalent ion in $Fe_{0.11}V_2O_{5.16}$ and $Cr_{0.11}V_2O_{5.16}$. The values indicated for the sol–gel V_2O_5 correspond to a fictive situation. (*b*) Ionic radii and M—O bond lengths after Shannon (ref. 24) ($r_{O^{2-}} = 1.22$ Å). (*c*) Values of atomic coordinates z of the different atoms (O, V, M) of the VO_6 polyhedron for $Fe_{0.11}V_2O_{5.16}$, $Cr_{0.11}V_2O_{5.16}$ and for sol–gel V_2O_5 (fictive situation).

(*a*)

	M—O2	M—O3	M—O4	M—O4′
$Fe_{0.11}V_2O_{5.16}$	2.151(7)	1.791(3)	1.98(2)	2.37(2)
$Cr_{0.11}V_2O_{5.16}$	2.081(8)	1.783(1)	2.14(3)	2.24(3)
V_2O_5	2.031	1.783	2.186	2.186

(*b*)

M^{3+}	coordination number	r/Å	d(M—O)/Å
Fe	6	0.79	2.01
	5	0.72	1.94
	4	0.63	1.85
Cr	6	0.76	1.98

(*c*)

	O2	O3	M	O4	O4′	V
$Fe_{0.11}V_2O_{5.16}$	0.989(2)	−0.001(2)	0.044(5)	1/2	−1/2	0.0950(5)
$Cr_{0.11}V_2O_{5.16}$	0.995(1)	0.005(2)	0.011(6)	1/2	−1/2	0.1055(5)
V_2O_5	0.996(2)	0.015(2)	0	1/2	−1/2	0.1082(6)

If we take into account the constraints due to the V_2O_5 framework leading to the invariance of the *b*-parameter, whatever the type of ion intercalated, it is clear that the distance M—O_3 (1.785 Å) is too short if compared to the theoretical bond length M—O (in the range 1.85 Å–2.01 Å) given in Table 5. However, the chromium ion occupies the most symmetrical available position [$d_{M—O4} = 2.14(3)$ Å, $d_{M—O4'} =$ 2.24(3) Å], consistent with an ideal octahedral environment ($d_{M—O4} = d_{M—O4'} = 2.19$ Å). This result can be easily explained by the high stabilization of Cr^{3+} in a high spin crystal field of octahedral symmetry. Since a high spin crystal field has no effect on the stabilization of a d^5 ion such as Fe^{3+} in an octahedral environment, the Fe^{3+} ion, which has an ionic radius ($r = 0.79$ Å) larger than Cr^{3+} ($r = 0.76$ Å), moves from the oxygen plane in order to increase the too short bond lengths M—O_3 (1.78 Å). This leads to a shortening of the M—O_4 bond perpendicular to the plane [1.98(2) Å *cf.* 2.37(2) Å for the other M—$O_{4'}$ bond]. Thus, Fe^{3+} adopts a distance ranging between five- ($d_{M—O} = 1.94$ Å) and six-coordination ($d_{M—O} = 2.01$ Å). The Fe^{3+} ion shows thus a tendency to a five-coordination, similarly to V^{5+} in V_2O_5 which is described by the association of layers built of VO_5 square pyramids rather than VO_6 octahedra.

Conclusion

In agreement with a previous study on the mixed iron vanadium oxide $Fe_{0.11}V_2O_{5.16}$, the structural results obtained by a Rietveld refinement of the $Cr_{0.11}V_2O_{5.16}$ structure confirm

that the V_2O_5 framework is preserved in these compounds, with a localization of the M^{3+} ion in the quasi-square plane formed by the four oxygen atoms of the V_2O_5 slab. Two oxygen atoms have to be added along with the M^{3+} ion, along the *c*-axis, in order to achieve an octahedral environment. However, the position of the M^{3+} ion along the *c* direction depends upon the nature of the inserted ion. The substantial crystal field stabilization for Cr^{3+} can explain its quasi-regular six-coordination, whereas the size effect in the case of Fe^{3+} brings it out of the oxygen plane and it tends to adopt five-coordination as for V^{5+} in V_2O_5 oxide.

The formation of short MO_6 octahedra chains linking the V_2O_5 layers in the $M_{0.11}V_2O_{5.16}$ compounds ($M = Fe^{3+}$, Cr^{3+}) increases their three-dimensional character. The presence of M^{3+} ions within the slabs of V_2O_5 prevents deformation of the framework during electrochemical insertion of lithium expected for a composition of *ca.* one lithium per vanadium atom.[25] This explains the better stability of the structural framework observed during lithium electrochemical cycling. A closely related discharge behavior has been reported for another sol–gel mixed oxide, the aluminium compound $Al_{0.11}V_2O_{5.16}$,[26] but with lower performances in term of cycling properties. Structural investigations are in progress concerning this compound for which it should be observed there is a stronger tendency to a five-coordination, insofar as the size of Al^{3+} ion ($r = 0.65$ Å) is clearly smaller than the size of Fe^{3+} or Cr^{3+} (0.79 Å). NMR investigations will be also carried out for this compound in order to confirm the X-ray diffraction results.

The authors are grateful to Dr. Pereira-Ramos (CNRS Thiais) for his fruitful comments concerning the electrochemical properties of V_2O_5-based materials.

References

1 J. Livage, M. Henry and C. Sanchez, *Prog. Solid State Chem.*, 1988, **18**, 259.
2 J. Livage, *L'Actualité Chimique*, 1997, **10**, 4.
3 J. Livage, *Chem. Mater.*, 1991, **3**, 579.
4 J. P. Pereira-Ramos, N. Baffier and G. Pistoia, in *Lithium Batteries, New Materials, Developments and Perspectives*, ed. G. Pistoia, Independent Chemical Library, Elsevier, Amsterdam, 1994, vol. 5, p. 281.
5 S. Maingot, R. Baddour, J. P. Pereira-Ramos, N. Baffier and P. Willmann, *J. Electrochem. Soc.*, 1993, **140**, L158.
6 J. Farcy, S. Maingot, P. Soudan, J. P. Pereira-Ramos and N. Baffier, *Solid State Ionics*, 1997, **99**, 61.
7 S. Maingot, P. Deniard, N. Baffier, J. P. Pereira-Ramos, A. Kahn-Harari, R. Brec and P. Willmann, *J. Power Sources*, 1995, **54**, 342.
8 B. Pecquenard, PhD Thesis, Université Paris VI, 1995.
9 P. Soudan, G. Grégoire, N. Baffier and J. P. Pereira-Ramos, *Ionics*, 1997, **3**, 261.
10 J. Lemerle, N. Nejem and J. Lefebvre, *J. Inorg. Nucl. Chem.*, 1980, **42**, 17.
11 P. Aldebert, N. Baffier, N. Gharbi and J. Livage, *Mater. Res. Bull.*, 1981, **16**, 669.
12 J. J. Legendre, P. Aldebert, N. Baffier and J. Livage, *J. Solid State Chem.*, 1982, **3**, 695.
13 J. J. Legendre and J. Livage, *J. Colloid Interface Sci.*, 1983, **94**, 75.
14 T. Yao, Y. Oka and N. Yamamoto, *Mater. Res. Bull.*, 1992, **27**, 669.
15 A. Bouhaouss, P. Aldebert, N. Baffier and J. Livage, *Rev. Chim. Miner.*, 1985, **22**, 417.
16 N. Baffier, L. Znaidi and J. C. Badot, *J. Chem. Soc., Faraday Trans.*, 1990, **86**, 2623.
17 M. Evain, U-FIT: A cell parameter refinement program, I. M. N. Nantes, France, 1992.
18 H. M. Rietveld, *J. Appl. Crystallogr.*, 1969, **2**, 65.
19 J. Rodriguez-Carvajal, in *Collected Abstract of Powder Diffraction Meeting*, Toulouse, France, 1990, p. 127.
20 G. Caglioti, A. Paoletti and F. P. Ricci, *Nucl. Instrum. Methods*, 1958, **35**, 223.
21 G. S. Pawley, *J. Appl. Crystallogr.*, 1981, **14**, 357.
22 R. Enjalbert and J. Galy, *Acta Crystallogr., Sect. C*, 1986, **42**, 1467.
23 H. G. Bachman, F. R. Ahmed and W. H. Barnes, *Z. Kristallogr.*, 1961, **115**, 110.
24 R. D. Shannon, *Acta Crystallogr., Sect. A*, 1976, **32**, 751.
25 J. M. Cocciantelli, J. P. Doumerc, M. Pouchard, M. Broussely and J. Labat, *J. Power Sources*, 1991, **34**, 103.
26 R. Baddour-Hadjean, J. Farcy, J. P. Pereira-Ramos and N. Baffier, *J. Electrochem. Soc.*, 1996, **143**, 2083.

Paper 8/01385C; *Received* 18*th February*, 1998